AGU PUBLICATIONS

Radio Science

RESEARCH ARTICLE
10.1002/2014RS005406

Special Section:
Beacon Satellite Symposium 2013

Effects of transionospheric signal decorrelation on Global Navigation Satellite Systems (GNSS) performance studied from irregularity dynamics around the northern crest of the EIA

T. Das[1], B. Roy[2], and A. Paul[2]

[1]S.K. Mitra Center for Research in Space Environment, University of Calcutta, Calcutta, India, [2]Institute of Radio Physics and Electronics, University of Calcutta, Calcutta, India

Key Points:
- Irregularity dynamical information derived from VHF spaced aerial measurements
- Proxy indicators of GNSS performance degradation
- Prediction of GPS L band S4

Correspondence to:
A. Paul,
ashikpaul@aol.in

Citation:
Das, T., B. Roy, and A. Paul (2014), Effects of transionospheric signal decorrelation on Global Navigation Satellite Systems (GNSS) performance studied from irregularity dynamics around the northern crest of the EIA, *Radio Sci.*, *49*, 851–860, doi:10.1002/2014RS005406.

Received 26 FEB 2014
Accepted 25 AUG 2014
Accepted article online 27 AUG 2014
Published online 8 OCT 2014

Abstract Transionospheric satellite navigation links operate primarily at L band and are frequently subject to severe degradation of performances arising out of ionospheric irregularities. Various characteristic features of equatorial ionospheric irregularity bubbles like the drift velocity, characteristic velocity, decorrelation time, and decorrelation distance can be determined using spaced aerial measurements at VHF. These parameters measured at VHF from a station Calcutta situated near the northern crest of the Equatorial Ionization Anomaly (EIA) in the geophysically sensitive Indian longitude sector have been correlated with L band scintillation indices and GPS position accuracy parameters for identifying possible proxies to L band scintillations. Good correspondences have been observed between decorrelation times and distances at VHF with GPS S_4 and Position Dilution of Precision during periods of GPS scintillations ($S_4 > 0.3$) for February–April 2011, August–October 2011, and February–April 2012. A functional relation has been developed between irregularity drift velocity measured at VHF and S_4 at L band during February–April 2011, and validation of measured S_4 and predicted values performed during August–October 2011 and February–April 2012. Significant improvement in L band scintillation prediction and consequent navigational accuracy will result using such relations derived from VHF irregularity measurements which are much simpler and inexpensive.

1. Introduction

Vast majority of transionospheric satellite signal users at equatorial locations are adversely affected by the occurrence of ionospheric scintillations during postsunset hours of equinoctial months in the Indian longitude sector. Excellent review articles on equatorial ionospheric *F* region irregularities are available in literature [*Fejer and Kelley*, 1980]. Scattering of signals from these irregularities embedded in the ionosphere are obtained in the form of spread *F* on radar maps [*Woodman and La Hoz*, 1976; *Fejer and Kelley*, 1980]. Plasma depletions were first observed by the polar orbiting OGO-6 satellite [*Hanson and Sanatani*, 1973]. The irregularities, in the form of depletions, manifest as deep bite-outs in in situ density plots [*Kelley et al.,* 1976; *McClure et al.,* 1977] and cause scintillations in transionospheric satellite links [*Aarons*, 1982, 1993; *Basu and Basu*, 1976, 1985; *Basu and Whitney*, 1983]. *Kil and Heelis* [1998] have reported the global distribution of ionospheric irregularities from the Atmospheric Explorer-E (AE-E) satellite data. Both airglow observations and scintillations with orbiting satellites show that the irregularity clouds may split into several streams as one moves away from the equator [*Bhar et al.,* 1970]. Airglow observations with all-sky cameras establish that the irregularity clouds become narrower with latitude on both sides of the magnetic equator [*Weber et al.,* 1980]. Radar detection of plasma irregularities [*Woodman and La Hoz*, 1976] and satellite encounters with density depletions [*Burke et al.,* 1979] at altitudes well above the peak of the *F* layer indicated that linear description of the Rayleigh-Taylor (R-T) instability at equatorial latitudes were incomplete. Above the peak of the *F* layer, instead of slowing and decaying, the sharply depleted bubbles move upward at supersonic speeds and are regularly seen in the evening sector [*Hanson et al.,* 1997]. *Anderson and Haerendel* [1979] followed the development of the RT instability into the nonlinear regime and showed that plasma bubbles are indeed able to break into the topside ionosphere. Depending on the direction of the background **E**, they may move upward, downward, or stagnate. Long-term VHF scintillation observations from a station, Calcutta, situated near the northern crest of the Equatorial Ionization Anomaly (EIA) in the Indian longitude sector, have

©2014. American Geophysical Union. All Rights Reserved.

been discussed [*Chakraborty et al.,* 1999; *Ray and DasGupta*, 2007]. Effects of relative velocity between GPS satellite vehicle and drifting irregularities on receiver performance have been reported from the equatorial region [*Kintner et al.,* 2001, 2004; *DasGupta et al.,* 2006]. GPS phase scintillation measurements, associated cycle slips, and impact on receiver tracking loops have been reported in literature [*Carrano and Groves*, 2010; *Humphreys et al.,* 2010a, 2010b; *Moraes et al.,* 2011, 2014; *Roy et al.,* 2013]. Optical measurements related to the triggering and subsequent evolution of equatorial ionospheric irregularities are available in literature [*Mukherjee*, 2002; *Martinis and Mendillo*, 2007; *Taori et al.,* 2011]. The issue of day-to-day variability in ionospheric irregularity generation giving rise to equatorial scintillation has been discussed utilizing the global imagery provided by the Global Ultraviolet Imager (GUVI) onboard NASA's Thermosphere Ionosphere Mesosphere Energetics and Dynamics (TIMED) satellite [*Basu et al.,* 2009].

Some of the most intense postsunset ionospheric scintillations are encountered at locations around the northern crest of the Equatorial Ionization Anomaly (EIA) in the Indian longitude sector, and the occurrence morphology depends on season, longitude, solar cycle, and magnetic activity, and exhibits a high degree of variability from one night to the next [*Aarons*, 1982]. Extensive observations of scintillations have been reported from the geophysically sensitive Indian longitude sector involving Applications Technology Satellite-6 (ATS-6) and All India Coordinated Programme of Ionospheric and Thermospheric Studies (AICPITS) [*Chandra et al.,* 1979, 1993; *Rastogi et al.,* 1982, 1990; *Somayajulu et al.,* 1984; *Dabas and Reddy*, 1986; *Kumar et al.,* 2000]. Stations like Calcutta (latitude: 22.58°N longitude: 88.38°E geographic; magnetic dip: 32°N) experience intense, often saturated, scintillations at VHF and L band on a significant proportion of nights during the equinoxes. While L band scintillations are mostly limited to premidnight hours, cases of VHF scintillations extending up to early morning hours have been observed from this station [*Ray and DasGupta*, 2007]. Impacts of equatorial ionospheric scintillations on technological systems which depend on transionospheric radio signals is significant and constitute one of the most potent threats to their accuracy of performance [*Paul et al.,* 2011; *Roy et al.,* 2013].

The ionospheric irregularities produce amplitude scintillations which represent the ground diffraction pattern of the satellite signal. Amplitude of the scintillation fading at a particular frequency depends upon the spatial distribution and amplitude of the density irregularities. The fading time scales are determined by the spatial scale called the Fresnel scale length and the zonal drift velocity of the irregularity where the drift varies during scintillation. The fading rate of a signal is expressed in terms of the autocorrelation of a time series of the signal. The autocorrelation function is a measure of the rapidity with which a point on the time series is decoupled from the neighboring point.

Equatorial ionospheric scintillations affect Global Navigation Satellite Systems (GNSS) signals according to a well-defined inverse frequency dependence. When scintillations are weak ($S_4 < 0.6$), this variation is expressed by $S_4 \propto f^{-1.5}$, where S_4 is the amplitude scintillation index, defined as the ratio of standard deviation of signal intensity fluctuations and the average signal intensity, and f is the signal frequency. When scintillations are strong, the exponent of the frequency dependence decreases. At locations around the northern crest of the Equatorial Ionization Anomaly (EIA), intense ($S_4 > 0.6$) to saturated VHF scintillations are frequently observed during early evening hours whose intensity gradually decrease with the progress of the night and become moderate to weak around midnight and postmidnight hours. On the same night, L band scintillation intensity may range from intense to moderate mostly limited to premidnight hours. Thus, it may not be appropriate to indicate one fixed frequency exponent to express the inverse frequency dependence across different scattering regimes.

The ionospheric irregularities usually move in an eastward direction with the drift velocity progressively decreasing from high early evening values of 150–200 m/s to about 50 m/s around 22:00 LT. The drift velocity of these ionospheric irregularities may be determined using spaced aerial measurements [*Mitra*, 1949; *Briggs et al.,* 1950; *Bhattacharyya et al.,* 2001, 2003] which are relatively simple and inexpensive to establish at VHF compared to L band. Some of the other parameters related to irregularity dynamics which can be derived from spaced aerial measurements are the characteristic velocity of the irregularities and the decorrelation time or decorrelation distance. The characteristic velocity provides a measure of the randomness of the medium of propagation. Decorrelation time of the signals received across two antennas separated by a finite distance provide information on the rate of evolution of the irregularity structures.

L band signals are applied for navigation purposes by GPS, Differential GPS (DGPS), Satellite-Based Augmented System (SBAS) and Global Navigation Satellite System (GNSS) catering to diverse panoply of

©2014. American Geophysical Union. All Rights Reserved.

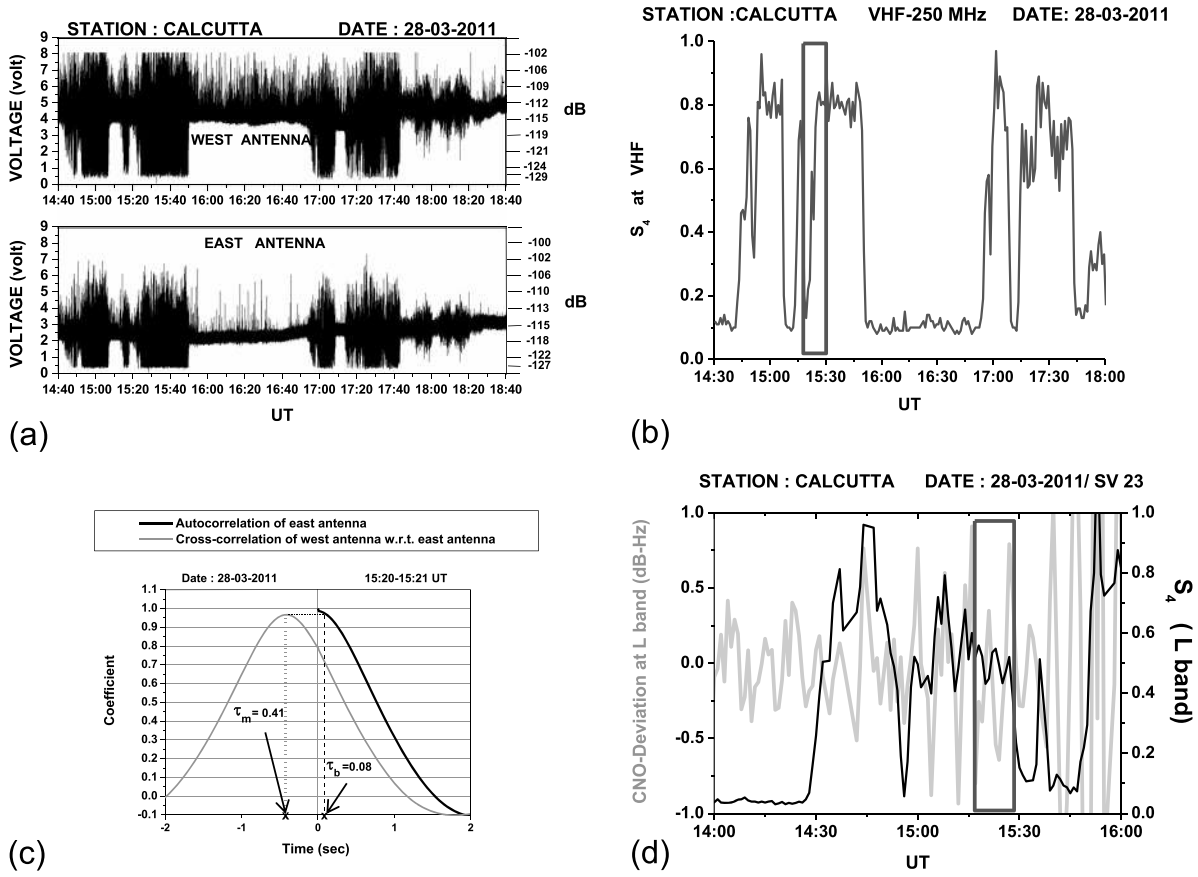

Figure 1. (a) Sample of VHF amplitude scintillations observed on the geostationary FSC link on two antennas aligned along geomagnetic east-west direction during 14:40–18:40 UT on 28 March 2011 at Calcutta. (b) Plot of S_4 index at VHF from FSC on 28 March 2011. (c) Plots of autocorrelation of the east antenna signal and cross correlation of the west antenna signal with respect to the east antenna signal during 15:20-15:21 UT. The values of τ_m and τ_p are indicated in the figure. (d) Corresponding variation of GPS SV23 S_4 index on 28 March 2011.

modern society. It is important to note that GNSS signal tracking becomes extremely difficult during periods of low decorrelation times thereby degrading the performances of SBAS [*Humphreys et al.,* 2005; *Moraes et al.,* 2011; *Akala et al.,* 2012]. Understanding the dependencies of irregularity mechanics at VHF and its possible implications on L band system forms a very important component of international space weather studies. Proxies to L band scintillations which affect SBAS could be obtained from VHF spaced aerial measurements, the latter being much simpler and inexpensive to install. Development of a functional relation between the measurements made at two frequencies may be effectively used for forecasting L band scintillation occurrences. The present paper reports the relation between irregularity motion parameters measured at VHF and their impact on GPS amplitude scintillations and position accuracy parameters like the Position Dilution of Precision (PDOP) measured from a station, Calcutta, situated virtually underneath the northern crest of the EIA in the geophysically sensitive Indian longitude sector over three equinoxes February–April 2011, August–October 2011, and February–April 2012. Validation of GPS measured S_4 with predicted values have been performed for a period outside the training data set using a relation developed between VHF irregularity dynamics and measured GPS S_4.

2. Data

VHF spaced aerial measurements have been recorded at Calcutta (22.58°N, 88.38°E geographic; magnetic dip: 32°N) using the geostationary FLEETSATCOM (Fleet Satellite Communications (FSC), 250 MHz, 350 km subionospheric point: 21.10°N, 87.25°E geographic; magnetic dip: 28.65°N) since August 2010 using wideband communication receivers. The receivers are calibrated once a week following *Basu and Basu* [1989].

©2014. American Geophysical Union. All Rights Reserved.

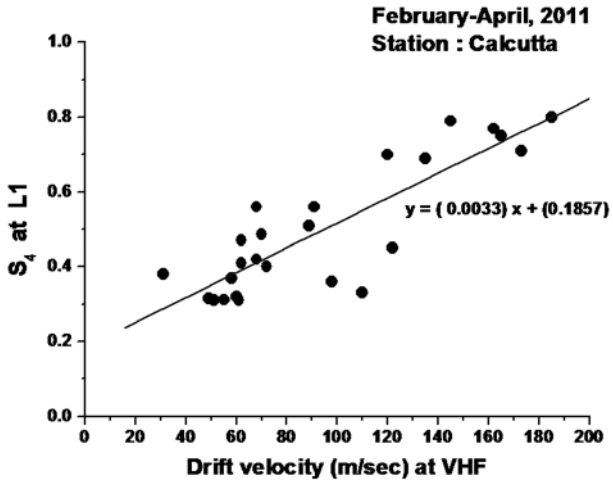

Figure 2. Variation of amplitude scintillation index S_4 at GPS L1 frequency with ionospheric irregularity drift velocity at VHF (250 MHz) measured from Calcutta during February through April 2011.

The dynamic range of each receiver is ~25 dB. The scintillation data were scaled to obtain Scintillation Index (SI (dB)) and S_4 following *Whitney et al.* [1969]. Stations like Calcutta situated at the northern crest of the Equatorial Ionization Anomaly (EIA) experience saturated VHF scintillations and intense ($S_4 > 0.6$) L band scintillations for a significant proportion of local postsunset to midnight hours during equinoctial months.

After the unusually prolonged bottom of the solar cycle spanning 2006–2010, scintillation activity dramatically picked up during the equinoxes of 2011. While the autumnal equinox of 2010 witnessed only a few cases of L band scintillations, 38 cases of intense ($S_4 > 0.6$) L band scintillations were recorded from Calcutta during February through April 2011. The corresponding numbers at L band were 22 during August through October 2011 and 25 during February through April 2012.

Spaced aerial measurements are one of the most popular methods for studying the dynamical characteristics of ionospheric irregularities. The nonfrozen aspects of the irregularities could be understood from an estimate of the drift velocity of the ground diffraction pattern. The characteristic velocity is taken as a measure of randomness of the medium of propagation. Decorrelation time indicates the rate of evolution of irregularities. Full Correlation Analysis [*Briggs et al.,* 1950; *Vacchione et al.,* 1987; *Bhattacharyya et al.,* 1989] technique has been used to determine the zonal drift and characteristics velocity of the irregularities transverse to the signal path. With the assumption that the amplitude space-time correlation function $C_A(x,t)$ is of the form

$$C_A(x,t) = f\left[(x - V_o t)^2 + V_c{}^2 t^2\right]$$

the "peak value" method shows that zonal drift velocity (V_o) and characteristic velocity (V_c) can be computed by using the following two formulas,

$$V_o = \Delta x\, \tau_m / \left(\tau_m{}^2 + \tau_p{}^2\right)$$

$$V_c{}^2 = \Delta x\ V_o/\tau_m - V_o{}^2$$

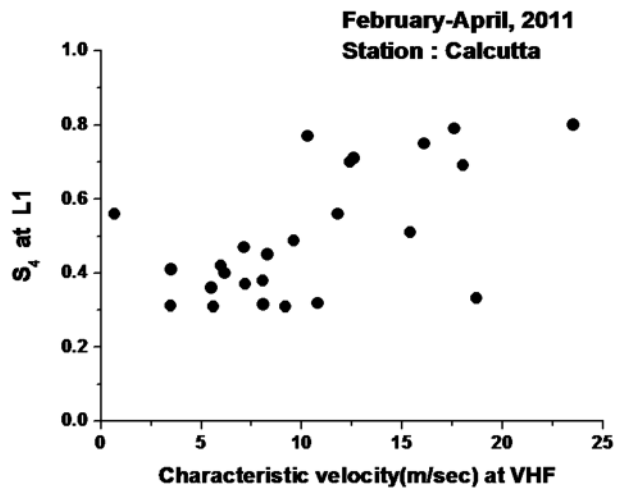

Figure 3. Variation of amplitude scintillation index S_4 at GPS L1 frequency with ionospheric irregularity characteristic velocity at VHF (250 MHz) measured from Calcutta during February through April 2011.

where Δx is the separation between two aerials aligned along geomagnetic east-west direction, τ_p is the time lag for which the autocorrelation of the amplitude equals the peak value of the cross-correlation function for the amplitudes recorded at the two receivers and τ_m is the time lag for which the cross-correlation function is maximum. The decorrelation time is calculated at 50% of τ_p. The decorrelation time is calculated with reference to the autocorrelation function of a single antenna, the east antenna in this case. The decorrelation distance is obtained from the product of the decorrelation time and the irregularity drift velocity. Detailed discussions of the

©2014. American Geophysical Union. All Rights Reserved.

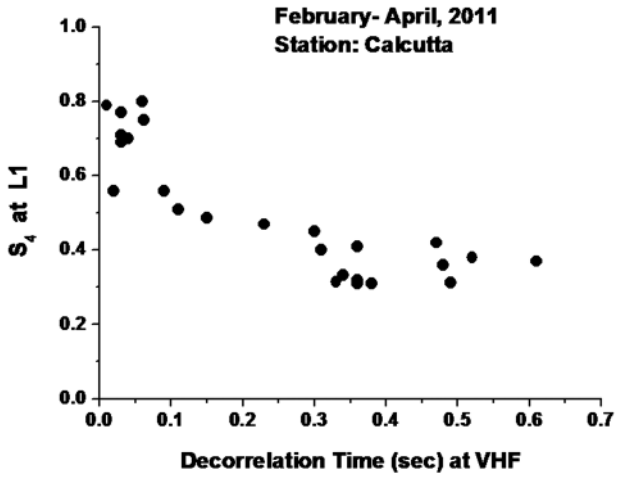

Figure 4. Variation of amplitude scintillation index S_4 at GPS L1 frequency with ionospheric irregularity decorrelation time at VHF (250 MHz) measured from Calcutta during February through April 2011.

equations and terms given above could be found in *Spatz et al.* [1988]. In the present paper, estimation of irregularity zonal drift velocities at VHF has been done during 20:00 LT to midnight in order to eliminate any contamination due to the vertical movement of the structure during the early phase of irregularity generation [*Kudeki and Bhattacharyya*, 1999]. It is important to note that irregularity zonal drift measurements show large dispersion at this time.

Dual-frequency GPS data recorded at Calcutta situated underneath the northern crest of the EIA have been used. For the analysis, GPS satellites observed from Calcutta with 350 km subionospheric points lying within latitude swath of 20.12°–22.12° and longitude 86.25°–88.25° were selected around that of FSC. The amplitude scintillation index S_4 and PDOP were logged at a sampling rate of 1 min. The received phase of the GPS signal at L1 frequency (1575.42 MHz) was sampled at 50 Hz and used for estimation of cycle slips from satellite links located within the above mentioned swath close to the 350 km subionospheric point of FSC following *Roy et al.* [2013]. Cycle slips on a particular GPS space vehicle (SV) link were estimated over the time period the receiver loses lock on the signal till it reacquires the signal. A causal understanding behind GNSS tracking errors at L band exceeding the specifications of International Civil Aviation Organization (ICAO) are being attempted using VHF measurements. In the present paper, cases of intense VHF scintillations with $S_4 > 0.6$ have been selected. During the correlation exercise with GPS L band scintillations, cases with GPS $S_4 > 0.3$ have been selected with corresponding subionospheric points lying within a swath close to that of FSC. However, there are several cases of GPS $S_4 > 0.6$ indicating intense scintillations.

The present paper reports (1) the results of correlation between VHF spaced aerial measurements and GPS L band scintillations indices for February–April 2011, August–October 2011, and February–April 2012, (2) examines the role of the decorrelation time on GNSS through the scintillation indices and position error parameters, and (3) validates predicted S_4 with measured values at GPS L1 frequency using a functional relationship developed using VHF irregularity drift velocity.

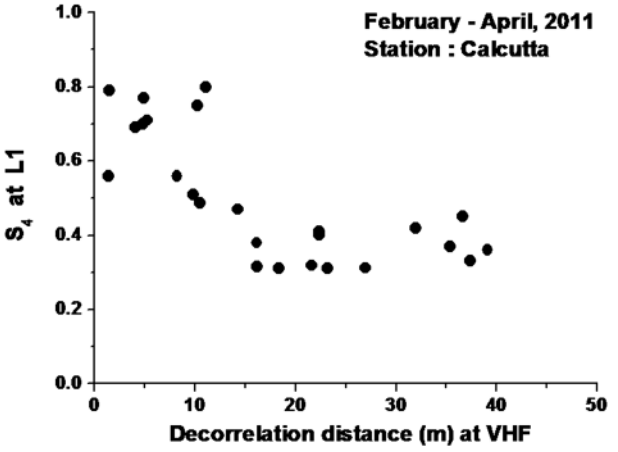

Figure 5. Variation of amplitude scintillation index S_4 at GPS L1 frequency with ionospheric irregularity decorrelation distances at VHF (250 MHz) measured from Calcutta during February through April 2011.

3. Results

During the three equinoxes of 2011 and 2012, it was found that the ionospheric irregularity drift velocities typically vary from 200 m/s in the early evening hours (19:00–21:00 LT) to about 50 m/s around midnight typically from west to east. Figure 1a shows a sample of VHF scintillation patches observed on the 250 MHz beacon from geostationary FSC affecting the west and the east antenna (aligned along geomagnetic east-west direction) during 14:40–18:40 UT on 28 March 2011. The signal strengths in decibels are also marked in the figure.

©2014. American Geophysical Union. All Rights Reserved.

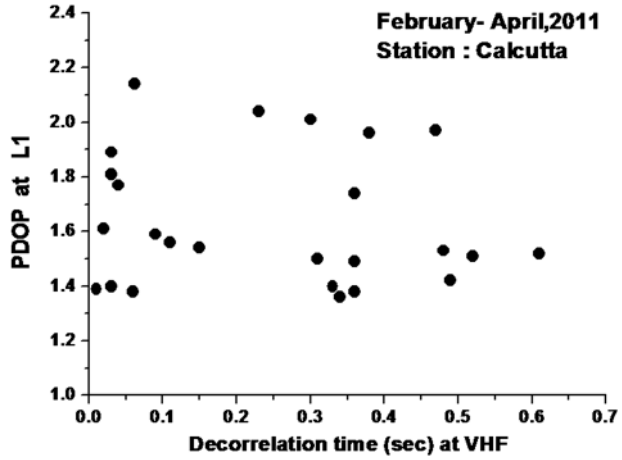

Figure 6. Correlation of Position Dilution of Precision (PDOP) for GPS with ionospheric irregularity decorrelation time at VHF (250 MHz) measured from Calcutta during February through April 2011.

The corresponding S_4 index at VHF is plotted in Figure 1b. The autocorrelation and cross-correlation function for a 1 min sample from 15:20–15:21 UT on 28 March 2011 from FSC is shown in Figure 1c. The times τ_p and τ_m are also indicated in the figure. Figure 1d shows the variation of S_4 index from GPS SV23 during 14:00–16:00 UT whose 350 km subionospheric point lies within a swath of ±1° around the subionospheric point of FSC. Similar plots of autocorrelation and cross correlation were generated for all the VHF scintillation patches observed on different days of the three equinoxes under consideration. Zonal drift velocities and characteristic velocities were calculated for each 1 min sample of scintillation patch observed on the FSC link each night using the method of Full Correlation Analysis. Decorrelation times and corresponding decorrelation distances were estimated based on 50% autocorrelation of the received signal on one antenna, the east antenna in this case. The necessity for spatial proximity of FSC and GPS SV subionospheric point is of prime importance in the present study. The number of data points was reduced when selecting GPS satellites whose 350 km subionospheric point lies close to that of FSC.

Figure 2 shows the relation between irregularity zonal drift velocity at VHF measured at Calcutta during February through April 2011 and the amplitude scintillation index S_4 at GPS L1 frequency for GPS SV links lying within ±1° of the subionospheric point of FSC. It is noted that higher irregularity drift velocities usually observed in the early evening hours correspond to high values of S_4, often saturated scintillations, at L band. Zonal drift velocities of 180–200 m/s are also noted in some cases. A linear equation was found, as shown in Figure 2, relating VHF irregularity drift velocity with GPS S_4. Characteristic velocities were calculated in order to understand the existence of any correspondence between randomness of the medium of propagation and intensity of transionospheric signal amplitude fluctuations. Variation of characteristic velocities at VHF with GPS L band S_4 is shown in Figure 3. Higher characteristic velocities at VHF are found to result in more intense amplitude scintillations at L band. Decorrelation of transionospheric satellite signals across two antennas separated by a distance are attributed to ionospheric scintillations and usually quantified in terms of decorrelation times and distances. These two parameters indicate the rapidity (both temporal and spatial) with which an ionospheric irregularity structure evolves. Figure 4 shows the calculated decorrelation times at VHF and corresponding GPS S_4 at L band. Low decorrelation times at VHF are found to be associated with periods of intense L band scintillations. It is important to note that decorrelation times at VHF less than 0.3 s are found to cause GPS L band scintillations with $S_4 > 0.4$. The decorrelation distance is found to be less than 10 m during periods of intense GPS scintillations ($S_4 > 0.6$) as shown in Figure 5. Such short decorrelation times and distances are issues of serious concern

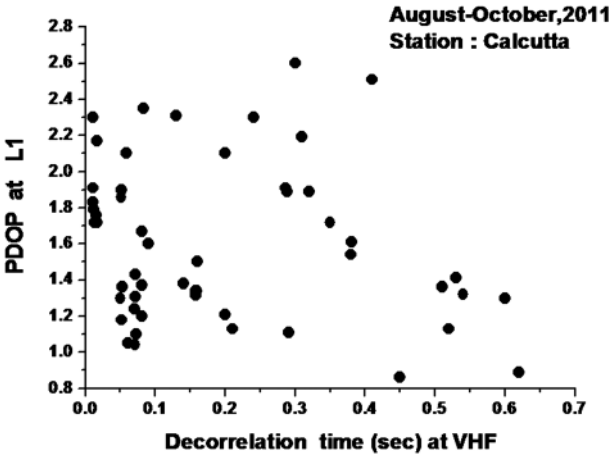

Figure 7. Correlation of Position Dilution of Precision (PDOP) for GPS with ionospheric irregularity decorrelation time at VHF (250 MHz) measured from Calcutta during August through October 2011.

©2014. American Geophysical Union. All Rights Reserved.

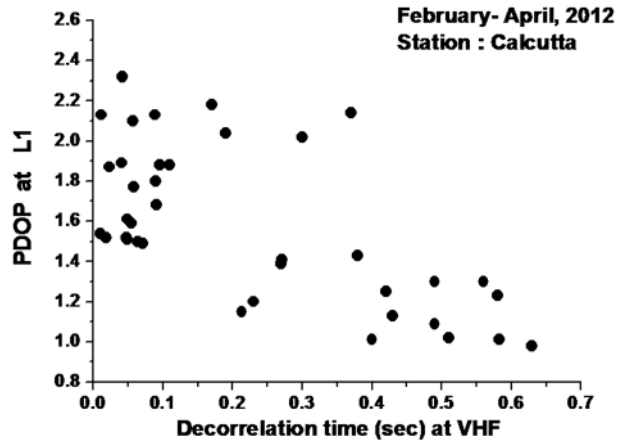

Figure 8. Correlation of Position Dilution of Precision (PDOP) for GPS with ionospheric irregularity decorrelation time at VHF (250 MHz) measured from Calcutta during February through April 2012.

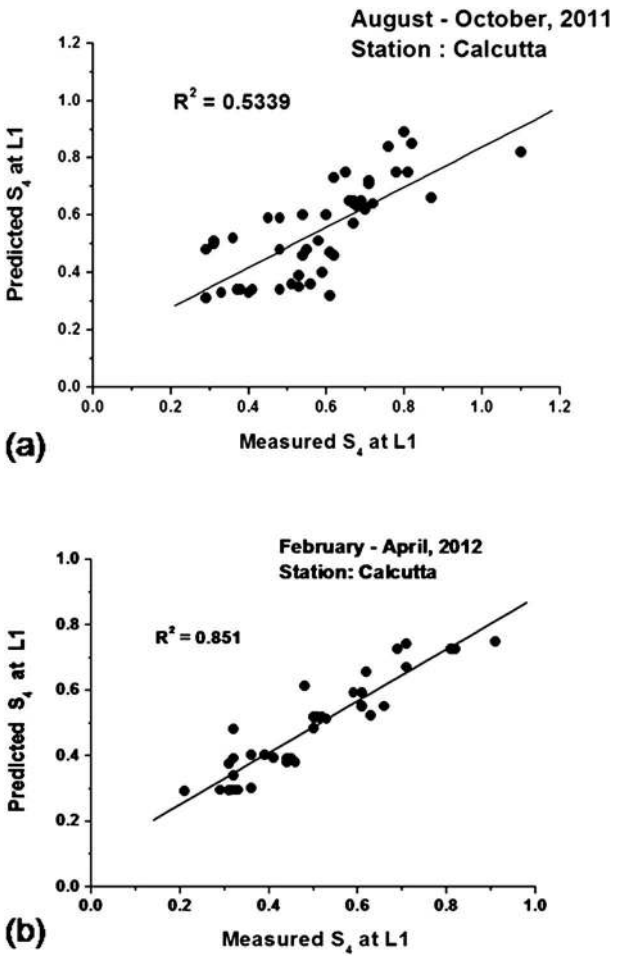

Figure 9. Comparison of measured and predicted GPS S_4 at L1 frequency during (a) August–October 2011 and (b) February–April 2012.

to SBAS system designers as these figures indicate significant deviations in transionospheric signal characteristics even across relatively short time periods and subionospheric points, during intense scintillations and calls for review of SBAS grid sizes as specified by the International Civil Aviation Organization (ICAO). In order to highlight the critical compromise of GPS position accuracy under intense ionospheric scintillations as frequently encountered at locations around the northern crest of the EIA in the Indian longitude sector, GPS PDOP values were studied corresponding to VHF decorrelation times. Identification of a proxy to position degradation of GNSS under adverse ionospheric conditions could be understood from VHF measurements as shown in Figure 6. It is observed that higher decorrelation times at VHF indicating less intense scintillations result in lower values of Position Dilution of Precision (PDOP) closer to 1.0 in GPS and hence better positioning accuracy. Values of PDOP around 1.0–1.2 are associated with decorrelation time of about 0.7 s. The associated cycle slips in the received phase of the L1 signal were calculated for SV links around the 350 km subionospheric point of FSC. High values of cycle slips of nearly 161 s [*Roy et al.,* 2013] were noted corresponding to decorrelation time of 0.1 s and PDOP of 2.2.

Similar exercises were performed during the autumnal equinox of 2011 and the vernal equinox of 2012. Figure 7 shows the variation of PDOP of GPS with decorrelation times at VHF during August through October 2011 and Figure 8 during February through April 2012, respectively. During August through October 2011, GPS PDOP values of 2.4 and cycle slips of ~23 s were found to correspond to VHF decorrelation time of 0.1 s indicating severe degradation of position accuracy. During February–April 2012, GPS PDOP values greater than 2.0 were found to correspond to VHF decorrelation time of 0.1 s.

From the plot of VHF zonal drift velocities and GPS S_4 measured during February through April 2011, a functional relation was developed between the two based on

©2014. American Geophysical Union. All Rights Reserved.

a trend line as shown in Figure 2. Using this equation, values of GPS S_4 were estimated for August–October 2011 and February–April 2012. In order to remove the bias of the data set used in developing the equation, validation of measured GPS S_4 was done with predicted values using this equation for other equinoxes, namely, during August through October 2011 and February–April 2012 as shown in Figures 9a and 9b, respectively. Closer correspondence is noted between the measured and predicted S_4 values during February through April 2012 with a regression coefficient of 0.85 than August through October 2011 which shows a regression coefficient of 0.53. This equation can be used as a proxy indicator for GPS scintillations. It should be noted that regression coefficients indicate the level of correlation and not causation at all times, between a dependent and an independent variable.

4. Summary and Conclusions

Although significant work have been conducted on irregularity dynamics and their modeling across different frequencies [*Franke and Liu*, 1983; *Bhattacharyya et al.,* 2001; *Carrano et al.,* 2011, 2012; *McNamara et al.,* 2013], correlation of the irregularity zonal movement parameters at VHF with L band ionospheric scintillations could result in significant improvement of system performance of transionospheric navigation systems operating at L band around the northern crest of the EIA. Significant decorrelation in received transionospheric satellite signal phase from C/NOFS has been reported at VHF and UHF from Ascension Island [*van de Kamp et al.,* 2010]. Correlation between the fading rates of VHF scintillations and GPS S_4 has been attempted earlier [*Das et al.,* 2010]. GPS PDOP, which combines values of horizontal as well as vertical positioning accuracies, provides an estimate of the level of integrity of position determination to the user. The evening equatorial ionosphere present very stringent conditions for transionospheric satellite systems, as the irregularities generated are often found to evolve at a very fast rate even across short baselines ~50–100 m resulting in low decorrelation times and high characteristic velocities. VHF signals are found to be decorrelated even across baselines of 10 m when GPS S_4 are in excess of 0.4 indicating strong scattering of the signals. It is found that periods of low decorrelation times at VHF ~ 0.1–0.2 s corresponded to intense L band scintillations ($S_4 > 0.6$ at L1 frequency) and high values of PDOP (2.0–2.4) indicating significant compromise of navigational accuracy. The received phase of the GPS signal at L1 exhibited cycle slips with high values of nearly 161 s during February through April 2011 and 23 s during August through October 2011 [*Roy et al.,* 2013]. These values are significantly higher than those specified by the International Civil Aviation Organization (ICAO) for application to high dynamic platforms like airplanes. Better correspondence between measured and predicted S_4 during February–April 2012 than August–October 2011 indicates seasonal dependence of ionospheric irregularity dynamical properties.

The meridional winds have been suggested to influence growth of equatorial ionospheric irregularities. The equatorial ionization anomaly has been found to exhibit asymmetry, both in terms of the locations of the northern and the southern crests as well as the ionization densities at the crests. The influence of a transequatorial wind appears to depress the *F* layer in the lee side hemisphere and to raise it in the windward hemisphere [*Rishbeth,* 1972; *Bittencourt and Sahai*, 1978]. Primarily, strong meridional winds are capable of creating this asymmetry in the equatorial ionization anomaly in the Northern and Southern Hemispheres. It would also facilitate significant changes in the *E* region conductivities that could control the *F* region dynamics. This in turn would be reflected in the postsunset *F* region height rise and eventually in the occurrence of scintillations. The above mechanism suggested by *Maruyama and Matuura* [1984] would operate irrespective of the winds being northward or southward. Latitudinal distribution of ionization density measured by Defense Meteorological Satellite Program (DMSP) could be used to estimate different parameters related to the asymmetry [*Paul and DasGupta*, 2010]. The relation between VHF irregularity drift velocity and GPS S_4 was derived for February–April 2011 and applied for validation over a different data set in August–October 2011 and February–April 2012. The equinoctial asymmetry in ionization has been suggested to be induced by variation in the O/N_2 ratio [*DasGupta et al.,* 1983]. It has also been suggested that the seasonal difference in scintillation occurrences are linked to changes of the integrated *E* region Pedersen conductivity [*Tsunoda*, 1985]. These factors may be responsible for better correspondence between measured and predicted GPS S_4 during February–April 2012 compared to August–October 2011.

From a statistical analysis of the drift velocities [*Otsuka et al.,* 2006], the eastward component of drift velocity just after sunset is found to be greater during March and April than during September and October. The present study tries to evolve a causal understanding between irregularity dynamics at VHF and its consequent

©2014. American Geophysical Union. All Rights Reserved.

effects on transionospheric L band signals and system. Significant advantage will accrue as a result of the applicability of relatively simple and inexpensive VHF measurements for prediction of L band scintillations affecting users of transionospheric satellite signals and system.

Acknowledgments
This research has been sponsored in part by the (1) Indian Space Research Organization (ISRO) through Research Projects at the S.K. Mitra Center for Research in Space Environment, University of Calcutta, Calcutta, India, (2) Centre of Advanced Study (CAS) at the Institute of Radio Physics and Electronics, University of Calcutta, Calcutta, India, (3) Technical Education Quality Improvement Program (TEQIP), University of Calcutta, Calcutta, India, and (4) the SCINDA program of the U.S. Air Force through the Asian Office of Aerospace Research and Development (AOARD). One of the authors (T.D.) acknowledges the support provided by Indian Space Research Organization (ISRO) through Research Fellowships at the S.K. Mitra Center for Research in Space Environment, University of Calcutta, Calcutta, India.

References

Aarons, J. (1982), Global morphology of ionospheric scintillations, *Proc. IEEE*, *70*(4), 360–378.
Aarons, J. (1993), The longitudinal morphology of equatorial *F*-layer irregularities relevant to their occurrence, *Space Sci. Rev.*, *63*(3–4), 209–243.
Akala, A. O., P. H. Doherty, C. S. Carrano, C. E. Valladares, and K. M. Groves (2012), Impacts of ionospheric scintillations on GPS receivers intended for equatorial aviation applications, *Radio Sci.*, *47*, RS4007, doi:10.1029/2012RS004995.
Anderson, D. N., and G. Haerendel (1979), The motion of depleted plasma regions in the equatorial ionosphere, *J. Geophys. Res.*, *84*, 4251–4256, doi:10.1029/JA084iA08p04251.
Basu, S., and S. Basu (1976), Correlated measurements of scintillations and in situ *F* region irregularities from OGO-6, *Geophys. Res. Lett.*, *3*, 681–684, doi:10.1029/GL003i011p00681.
Basu, S., and S. Basu (1985), Equatorial scintillations: Advances since ISEA-6, *J. Atmos. Terr. Phys.*, *47*(8), 753–768.
Basu, S., and S. Basu (1989), Scintillation technique for probing ionospheric irregularities, in *World Ionospheric Thermospheric Studies (WITS) Handbook*, vol. 2, edited by C. H. Liu, pp. 128–136, SCOSTEP, Univ. of Ill., Urbana, Ill.
Basu, S., and H. E. Whitney (1983), The temporal structure of intensity scintillations near the magnetic equator, *Radio Sci.*, *18*, 263–271, doi:10.1029/RS018i002p00263.
Basu, S., S. Basu, J. Huba, J. Krall, S. E. McDonald, J. J. Makela, E. S. Miller, S. Ray, and K. Groves (2009), Day-to-day variability of the equatorial ionization anomaly and scintillations at dusk observed by GUVI and modeling by SAMI3, *J. Geophys. Res.*, *114*, A04302, doi:10.1029/2008JA013899.
Bhar, J. N., A. DasGupta, and S. Basu (1970), Studies on *F*-region irregularities at low latitude from scintillations of satellite signals, *Radio Sci.*, *5*, 939–942, doi:10.1029/RS005i006p00939.
Bhattacharyya, A., S. J. Franke, and K. C. Yeh (1989), Characteristic velocity of equatorial *F* region irregularities determined from spaced receiver scintillation data, *J. Geophys. Res.*, *94*, 11,959–11,969, doi:10.1029/JA094iA09p11959.
Bhattacharyya, A., S. Basu, K. M. Groves, C. E. Valladares, and R. Sheehan (2001), Dynamics of equatorial *F* region irregularities from spaced receiver scintillation observations, *Geophys. Res. Lett.*, *28*, 119–122, doi:10.1029/2000GL012288.
Bhattacharyya, A., K. M. Groves, S. Basu, and H. Kuenzler (2003), L-band scintillation activity and space-time structure of low-latitude UHF scintillations, *Radio Sci.*, *38*(1), 1004, doi:10.1029/2002RS002711.
Bittencourt, J. A., and Y. Sahai (1978), *F*-region neutral winds from ionosonde measurements of *hmF2* at low latitude magnetic conjugate region, *J. Atmos. Terr. Phys.*, *40*(6), 669–676.
Briggs, B. H., G. J. Phillips, and D. H. Shinn (1950), The analysis of observations on spaced receivers of the fading of radio signals, *Proc. Phys. Soc. B*, *63*, 106, doi:10.1088/0370-1301/63/2/305.
Burke, W. J., D. E. Donatelli, R. C. Sagalyn, and M. C. Kelley (1979), Observations of low density regions at high altitudes in the topside equatorial ionosphere and their interpretation in terms of equatorial spread-*F*, *Planet. Space Sci.*, *27*(5), 593–601.
Carrano, C. S., and K. M. Groves (2010), Temporal decorrelation of GPS satellite signals due to multiple scattering from ionospheric irregularities, in *Proceedings of the 2010 Institute of Navigation ION GNSS Meeting*, pp. 361–374, Institute of Navigation, Portland, Oreg.
Carrano, C. S., K. M. Groves, R. G. Caton, C. L. Rino, and P. R. Straus (2011), Multiple phase screen modeling of ionospheric scintillation along radio occultation raypaths, *Radio Sci.*, *46*, RS0D07, doi:10.1029/2010RS004591.
Carrano, C. S., K. M. Groves, and R. G. Caton (2012), The effect of phase scintillations on the accuracy of phase screen simulation using deterministic screens derived from GPS and ALTAIR measurements, *Radio Sci.*, *47*, RS0L25, doi:10.1029/2011RS004958.
Chakraborty, S. K., A. DasGupta, S. Ray, and S. Banerjee (1999), Long-term observations of VHF scintillation and total electron content near the crest of the equatorial anomaly in the Indian longitude zone, *Radio Sci.*, *34*, 241–255, doi:10.1029/98RS02576.
Chandra, H., H. O. Vats, M. R. Deshpande, R. G. Rastogi, G. Sethia, J. H. Sastri, and B. S. Murthy (1979), Ionospheric scintillations associated with features of equatorial ionosphere, *Ann. Geophys.*, *35*, 145–151.
Chandra, H., et al. (1993), Coordinated multistation VHF scintillations observations in India during March–April 1991, *Indian J. Radio Space Phys.*, *22*, 69–81.
Dabas, R. S., and B. M. Reddy (1986), Night time VHF scintillations at 23°N magnetic latitude and their association with equatorial *F*-region irregularities, *Radio Sci.*, *21*, 453–462, doi:10.1029/RS021i003p00453.
Das, A., A. DasGupta, and S. Ray (2010), Characteristics of L-band (1.5 GHz) and VHF (244 MHz) amplitude scintillations recorded at Kolkata during 1996–2006 and development of models for the occurrence probability of scintillations using Neural network, *J. Atmos. Sol. Terr. Phys.*, *72*(9–10), 685–704.
DasGupta, A., D. N. Anderson, and J. A. Klobuchar (1983), Equatorial *F*-region ionization differences between March and September, 1979, *Adv. Space Res.*, *2*(10), 199–202.
DasGupta, A., A. Paul, S. Ray, A. Das, and S. Ananthakrishnan (2006), Equatorial bubbles as observed with GPS measurements over Pune, India, *Radio Sci.*, *41*, RS5S28, doi:10.1029/2005RS003359.
Fejer, B. G., and M. C. Kelley (1980), Ionospheric irregularities, *Rev. Geophys. Space Phys.*, *18*(2), 401–454.
Franke, S. J., and C. H. Liu (1983), Observations and modeling of multifrequency VHF and GHz scintillations in the equatorial region, *J. Geophys. Res.*, *88*, 7075–7085, doi:10.1029/JA088iA09p07075.
Hanson, W. B., and S. Sanatani (1973), Large N_i gradients below the equatorial *F*-peak, *J. Geophys. Res.*, *78*, 1167–1173, doi:10.1029/JA078i007p01167.
Hanson, W. B., W. R. Coley, R. A. Heelis, and A. L. Urquhart (1997), Fast equatorial bubbles, *J. Geophys. Res.*, *102*, 2039–2046, doi:10.1029/96JA03376.
Humphreys, T. E., M. L. Psiaki, B. M. Ledvina, and P. M. Kintner (2005), GPS carrier tracking loop performance in the presence of ISs, Proc. ION GNSS 2005, Institute of Navigation, Long Beach, Calif.
Humphreys, T. E., M. L. Psiaki, B. M. Ledvina, A. P. Cerruti, and P. M. Kintner Jr. (2010a), Data-driven testbed for evaluating GPS carrier tracking loops in ionospheric scintillation, *IEEE Trans. Aerosp. Electron. Syst.*, *46*(4), 1609–1623.
Humphreys, T. E., M. L. Psiaki, and P. M. Kintner (2010b), Modeling the effects of ionospheric scintillation on GPS carrier phase tracking, *IEEE Trans. Aerosp. Electron. Syst.*, *46*(4), 1624–1637.

©2014. American Geophysical Union. All Rights Reserved.

Kelley, M. C., G. Haerendal, H. Kappler, A. Valenzuela, B. B. Balsley, D. A. Carter, W. L. Ecklund, C. W. Carlson, B. Hausler, and R. Torbert (1976), Evidence for a Rayleigh-Taylor type instability and upwelling of depleted density regions during equatorial spread-*F*, *Geophys. Res. Lett.*, *3*, 448–450, doi:10.1029/GL003i008p00448.

Kil, H., and R. A. Heelis (1998), Global distribution of density irregularities in the equatorial ionosphere, *J. Geophys. Res.*, *103*, 407–417, doi:10.1029/97JA02698.

Kintner, P. M., H. Kil, T. L. Beach, and E. R. de Paula (2001), Fading timescales associated with GPS signals and potential consequences, *Radio Sci.*, *36*, 731–743, doi:10.1029/1999RS002310.

Kintner, P. M., B. M. Ledvina, E. R. de Paula, and I. J. Kantor (2004), Size, shape, orientation, speed, and duration of GPS equatorial anomaly scintillations, *Radio Sci.*, *39*, RS2012, doi:10.1029/2003RS002878.

Kudeki, E., and S. Bhattacharyya (1999), Post-sunset vortex in equatorial F-region plasma drifts and implications for bottomside spread-F, *J. Geophys. Res.*, *104*, 28,163–28,170, doi:10.1029/1998JA900111.

Kumar, S., et al. (2000), Coordinated observations of VHF scintillations in India during February–March, 1993, *Indian J. Radio Space Phys.*, *29*, 22–29.

Martinis, C., and M. Mendillo (2007), Equatorial spread F-related airglow depletions at Arecibo and conjugate observations, *J. Geophys. Res.*, *112*, A10310, doi:10.1029/2007JA012403.

Maruyama, T., and N. Matuura (1984), Longitudinal variability of annual changes in activity of equatorial spread-*F* and plasma bubbles, *J. Geophys. Res.*, *89*, 10,903–10,912, doi:10.1029/JA089iA12p10903.

McClure, J. P., W. B. Hanson, and J. H. Hoffman (1977), Plasma bubbles and irregularities in the equatorial ionosphere, *J. Geophys. Res.*, *82*, 2650–2656, doi:10.1029/JA082i019p02650.

McNamara, L. F., R. G. Caton, R. T. Parris, T. R. Pedersen, D. C. Thompson, K. C. Wiens, and K. M. Groves (2013), Signatures of equatorial plasma bubbles in VHF satellite scintillations and equatorial ionograms, *Radio Sci.*, *48*, 89–101, doi:10.1002/rds.20025.

Mitra, S. N. (1949), A radio method of measuring winds in the ionosphere, *Proc. Inst. Electr. Eng., Part 3*, *96*, 441–446.

Moraes, A. O., F. S. Rodrigues, W. J. Perrella, and E. R. Paula (2011), Analysis of the characteristics of low-latitude GPS amplitude scintillation measured during solar maximum conditions and implications for receiver performance, *Surv. Geophys.*, *33*(5), 1107–1131, doi:10.1007/s10712-011-9161-z.

Moraes, A. O., E. R. de Paula, M. T. de Assis Honorato Muella, and W. J. Perrella (2014), On the second order statistics for GPS ionospheric scintillation modeling, *Radio Sci.*, *49*, 94–105, doi:10.1002/2013RS005270.

Mukherjee, G. K. (2002), Mapping of the simultaneous movement of Equatorial Ionization Anomaly (EIA) and ionospheric plasma bubbles through all-sky imaging of OI 630 nm emission, *Terr. Atmos. Oceanic Sci.*, *13*, 53–64.

Otsuka, Y., K. Shiokawa, and T. Ogawa (2006), Equatorial ionospheric scintillations and zonal irregularity drifts observed with closely spaced GPS receivers in Indonesia, *J. Meteorol. Soc. Jpn.*, *84A*, 343–351.

Paul, A., and A. DasGupta (2010), Characteristics of the equatorial ionization anomaly in relation to the day-to-day variability of ionospheric irregularities around the postsunset period, *Radio Sci.*, *45*, RS6001, doi:10.1029/2009RS004329.

Paul, A., B. Roy, S. Ray, A. Das, and A. DasGupta (2011), Characteristics of intense space weather events as observed from a low latitude station during solar minimum, *J. Geophys. Res.*, *116*, A10307, doi:10.1029/2010JA016330.

Rastogi, R. G., H. Chandra, and M. R. Deshpande (1982), Equatorial scintillations of ATS-6 radio beacons: Phase II-Ootacamund 1975-76, *Indian J. Radio Space Phys.*, *11*, 240–246.

Rastogi, R. G., P. V. Koparkar, H. Chandra, and M. R. Deshpande (1990), Multifrequency studies of equatorial ionospheric scintillations at Ootacamund, *J. Atmos. Terr. Phys.*, *52*, 69–76.

Ray, S., and A. DasGupta (2007), Geostationary L-band signal scintillation observations near the crest of equatorial anomaly in the Indian zone, *J. Atmos. Sol. Terr. Phys.*, *69*(4–5), 500–514.

Rishbeth, H. (1972), Thermospheric winds and the *F*-region: A review, *J. Atmos. Terr. Phys.*, *34*(1), 1–47.

Roy, B., A. DasGupta, and A. Paul (2013), Impact of space weather events on satellite-based navigation, *Space Weather*, *11*, 680–686, doi:10.1002/2013SW001001.

Somayajulu, Y. V., S. C. Garg, R. S. Dabas, L. Singh, T. R. Tyagi, B. Loknadhan, S. Ramkrishna, and G. Navneeth (1984), Multistation study of night time scintillations in low latitudes: Evidence of control by equatorial F region irregularities, *Radio Sci.*, *19*, 707–718, doi:10.1029/RS019i003p00707.

Spatz, D. E., S. J. Franke, and K. C. Yeh (1988), Analysis and interpretation of spaced receiver scintillation data recorded at an equatorial station, *Radio Sci.*, *23*, 347–361, doi:10.1029/RS023i003p00347.

Taori, A., N. Dashora, K. Raghunath, J. M. Russell III, and M. G. Mlynczak (2011), Simultaneous mesosphere-thermosphere-ionosphere parameter measurements over Gadanki (13.5°N, 79.2°E): First results, *J. Geophys. Res.*, *116*, A05310, doi:10.1029/2010JA016229.

Tsunoda, R. T. (1985), Control of seasonal and longitudinal occurrence of equatorial scintillations by the longitudinal gradient in integrated *E*-region Pedersen conductivity, *J. Geophys. Res.*, *90*, 447–456, doi:10.1029/JA090iA01p00447.

Vacchione, J. D., S. J. Franke, and K. C. Yeh (1987), A new analysis technique for estimating zonal irregularity drifts and variability in the equatorial *F* region using spaced receiver scintillation data, *Radio Sci.*, *22*, 347–361, doi:10.1029/RS022i005p00745.

van de Kamp, M., P. S. Cannon, and R. J. Watson (2010), V/UHF space radars: Spatial phase decorrelation of transionospheric signals in the equatorial region, *Radio Sci.*, *45*, RS4012, doi:10.1029/2009RS004226.

Weber, E. J., J. Buchau, and J. G. Moore (1980), Airborne studies of equatorial *F*-layer ionospheric irregularities, *J. Geophys. Res.*, *85*, 4631–4641, doi:10.1029/JA085iA09p04631.

Whitney, H. E., J. Aarons, and C. Malik (1969), A proposed index for measuring ionospheric scintillations, *Planet. Space Sci.*, *17*(5), 1069–1073.

Woodman, R. F., and C. La Hoz (1976), Radar observations of *F*-region equatorial irregularities, *J. Geophys. Res.*, *81*, 5447–5466, doi:10.1029/JA081i031p05447.

©2014. American Geophysical Union. All Rights Reserved.